Thermal Stability of Apolipoprotein B100 in Low-Density Lipoprotein Is Disrupted at Early Stages of Oxidation While Neutral Lipid Core Organization Is Conserved†

Ruth Prassl,*,‡ Bernhard Schuster,§ Peter Laggner,‡ Claudie Flamant,|| Fabienne Nigon,|| and M. John Chapman||

Institute of Biophysics and X-ray Structure Research of the Austrian Academy of Sciences, Steyrergasse 17/VI, A-8010 Graz, Austria, and INSERM Unite 321, Unite de Recherches sur les Lipoproteines et l'Atherogenese, Hôpital de la Pitié, 75654 Paris Cedex 13, France

Received July 29, 1997; Revised Manuscript Received November 10, 1997

ABSTRACT: The time course of the unfolding characteristics of the protein moiety and of the thermotropic behavior of the core-located apolar lipids of highly homogeneous low-density lipoprotein (LDL) subspecies (*d* 1.030−1.040 g/mL) have been evaluated during transition metal- and azo radical-induced oxidation using differential scanning calorimetry. Apolipoprotein B100 (apo-B100) structure was highly sensitive to oxidative modification; indeed, a significant loss of thermal stability was observed at initial stages irrespective of whether oxidation was mediated by site-specific binding of copper ions or by free radicals generated during decomposition of azo compounds. Subsequently, thermal protein integrity was destroyed, as a result of potentially irreversible protein unfolding, cross-linking reactions, and aggregation. Our results suggest that even minimal oxidative modification of apo-B100 has a major impact on the stability of this large monomeric protein. By contrast, the core lipids, which consist primarily of cholesteryl esters and triglycerides and play a determinant role in the thermal transition occurring near physiological temperature, preserved features of an ordered arrangement even during propagation of lipid peroxidation.

Extensive evidence is now available to substantiate the hypothesis that oxidative modification of both the lipid and the protein components of low-density lipoprotein (LDL)[1] plays a significant role in the initiation and progression of atherosclerosis *in vivo* (for reviews, see *1*−*5*). Recent studies have revealed that a number of physicochemical properties and more specifically, particle size (*6*−*8*), the intrinsic properties of the protein moiety (*9*), the degree of fatty acid unsaturation (*10*), the molecular packing of the core lipids (*11*), and the content of biological antioxidants (*12*) influence the susceptibility of LDL to oxidation and, in addition, the kinetics of the oxidative process.

LDL are quasi-spherical particles, organized into two major compartments, a hydrophobic core, comprised primarily of cholesteryl esters (CE) and minor amounts of triglycerides (TG), surrounded by a monolayer of phospholipids, unesterified cholesterol (*13*−*15*), and a single copy of apolipoprotein B100 (apo-B100); the latter, a large protein of 4536 amino acid residues, is embedded at the surface of this supramolecular complex. The core lipids of LDL undergo a reversible, thermal transition close to physiological temperature (*13*, *16*). Below this transition temperature, the core-located lipids are arranged in an ordered liquid-crystalline phase; above the transition temperature however, the neutral lipids are organized in a fluid, oil like, randomly distributed state (*16*−*18*).

Recently, it has become apparent that the core melting transition influences the susceptibility of polyunsaturated fatty acids (PUFAs) to oxidation (*11*). As a consequence, the question arises as to the time course of oxidative changes in the lipid and protein moieties of LDL upon initiation of the oxidation process. We have therefore investigated the effects of transition metal- and azo radical-mediated oxidation on the thermal stability of both the core-located lipids and the protein moiety of highly homogeneous particle subspecies of LDL by differential scanning calorimetry. Earlier studies have demonstrated that major alterations in both the lipid and the protein components of LDL characterize the advanced stages of oxidative modification, which include extensive degradation of PUFAs and loss of esterified cholesterol together with formation of malondialdehyde (MDA) and other aldehydic lipid peroxidation products (*19*); the latter substances in turn modify specific amino acid residues of apo-B100 (*20*, *21*), leading to cleavage and fragmentation of the protein backbone. Our present data, however, support the hypothesis that profound alterations in protein conformation and thermal stability of apo-B100

† This work was supported by the Fonds zur Förderung der wissenschaftlichen Forschung in Österreich (projects P 10105-MOB to P.L. and S07112-MED and P11697-MED to R.P.), by European Community Concerted Action (PL931790), by BIOMED II (PL950134), and by INSERM.

* To whom correspondence should be addressed.

‡ Institute of Biophysics and X-ray Structure Research of the Austrian Academy of Sciences.

§ Present address: Zentrum für Ultrastrukturforschung und Ludwig Boltzmann-Institut für Molekulare Nanotechnologie, Universität für Bodenkultur, Gregor-Mendel-Strasse 33, A-1180 Vienna, Austria.

|| INSERM Unite 321, Unite de Recherches sur les Lipoproteines et l'Atherogenese, Hôpital de la Pitié.

[1] Abbreviations: LDL, low-density lipoprotein(s); apo-B100, apolipoprotein B100; CE, cholesteryl ester; TG, triglyceride; EDTA, ethylenediaminetetraacetic acid disodium salt; TBARS, thiobarbituric acid-reactive substances; MDA, malondialdehyde; SDS, sodium dodecyl sulfate; PUFA, polyunsaturated fatty acid; AAPH, 2,2′-azobis(2-amidinopropane) dihydrochloride; DSC, differential scanning calorimetry.

S0006-2960(97)01853-9 CCC: $15.00
Published on Web 01/03/1998

occur at early stages of oxidative stress; in contrast, the thermally dependent structural organization of the core lipids remains stable for a prolonged period, despite high rates of bulk lipid peroxidation, as indicated by conjugated diene formation.

MATERIALS AND METHODS

Lipoprotein Isolation and Density Gradient Fractionation. LDL were isolated from the plasma of normolipidemic healthy volunteers and fractionated by isopycnic density gradient ultracentrifugation as described earlier (*22*). Highly homogeneous LDL subspecies of intermediate density (*d* 1.030−1.040 g/mL) were exhaustively dialyzed at 4 °C for 24 h against 10 mM phosphate buffer at pH 7.4, containing 150 mM NaCl, 270 μM EDTA, and 50 mg/L gentamycin. All buffers and solutions were saturated with argon after deoxygenation under vacuum. LDL preparations were stored in the dark at 4 °C in an argon atmosphere until use within 2 weeks. Immediately before initiation of oxidation, EDTA was removed by gel filtration (prepacked Econo-Pac 10DG columns, Bio-Rad). The chemical composition of the LDL subspecies was determined as described earlier (*23*) and found to be in agreement with previous data for human LDL subspecies of intermediate density [i.e., LDL-3 (*6*)].

Lipid Peroxidation. The time course of LDL oxidation and the degree of lipid peroxidation was determined by continuously monitoring the diene production profile (absorption at 234 nm) (*24*−*27*). At constant molar ratios of LDL to copper and LDL to AAPH of 1:17 and 1:10 000, respectively, the lag and propagation period together with diene accumulation were calculated according to established procedures (*28*). Measurements were performed in a double-beam spectrophotometer (Model U-2000; Hitachi, Japan) equipped with a thermostated six-position automatic sample changer. The temperature was adjusted to 37 °C. In addition, the extent of lipid peroxidation was measured as thiobarbituric acid-reactive substances (TBARS). LDL solutions (50 μg of protein/mL) were mixed with 0.5 mL of 10% trichloracetic acid and 1 mL of 0.67% thiobarbituric acid. After the sample was heated in a boiling water bath for 30 min, the optical density was determined at 532 nm. Freshly diluted samples of tetraethoxypropane, which yield MDA, were utilized as the calibration standard. The apparent generation of TBA-reactive material should be interpreted cautiously, since it is well-documented that the TBA assay is not specific for lipid peroxidation products (*29*, *30*). Therefore, within this study, the assay served solely as an index for progress of lipid peroxidation.

Lipid Analysis. The lipid composition and quantification of both native and oxidized LDL samples were determined by gas chromatography as previously described by Kuksis et al. (*31*) with some modifications. An aliquot of LDL solution (250 μg LDL) was digested with phospholipase C (*Candida welchii*). To the LDL was added 1 mL of diethyl ether, 1 mL of 1% $CaCl_2$, and 1 mL of a solution (35 mM Tris buffer, pH 7.3) containing 1 unit of phospholipase C. The reaction mixture was then treated with 5 drops of 0.1 N HCl and extracted once with 5 mL of chloroform−methanol, 2:1 (v/v), containing 50 μg of the internal standard (tridecanoylglycerol). The solvent phases were separated by centrifuging for 10 min at 200*g*. The lower clear chloroform phase was dried by passage through a Pasteur pipette containing 2 g of anhydrous Na_2SO_4, and the solvent was evaporated to dryness under a stream of nitrogen. The lipids were then reacted for 60 min at room temperature with 150 μL of Tri-Sil/BSA (Pierce). The analyses were done on a Model 5860 Series II gas chromatograph equipped with a hydrogen flame ionization detector (Hewlett-Packard, France), with a HP Model 7673A autosampler designed for on-column injection and with a HP Model 3396B integrator unit. The samples were chromatographed on a 25 cm × 0.53 mm ID column (SGE, France), with a film thickness of 0.15 μm and a siloxane−carborane copolymer phase. Two microliters of sample was injected on-column at 100 °C and then the column temperature was programmed as follows: 50 °C/min to 175 °C and then 4 °C/min to 350 °C. The carrier gas (helium) flow was 10 mL/min. The hydrogen flame ionization detector was maintained at 370 °C. The composition of the sample was calculated in relation to the internal standard. The peak identity and areas were evaluated using appropriate standards and calibration factors.

Oxidation Procedure for Calorimetric Experiments. To an EDTA-free LDL solution containing about 1 mg of LDL protein/mL in 10 mM phosphate-buffered saline at pH 7.4 was added an aliquot of a 17 μM $CuCl_2$ solution to attain a final concentration of 1.7 μM Cu^{2+}/250 μg of LDL. Azo radical-induced oxidation was initiated by adding aliquots of a 0.5 M 2,2′-azobis(2-amidinopropane) dihydrochloride (AAPH) solution, instead of copper, to achieve a final ratio of 10 mM or 20 mM AAPH/μM LDL. The buffer solutions had been stirred with Chelex 100 resin (Bio-Rad) to remove any contamination by transition metal ions.

In one experiment, ebselen (2-phenyl-1,1-benzisoselenazol-3(2*H*)-one; ICN Biochemicals Ltd., U.K.) was used to remove some preformed lipid hydroperoxides from native LDL (*32*). Ten microliters of 20 mM ebselen solution in ethanol was mixed with LDL (final concentration 30 μM ebselen/1 μM LDL) and incubated at 37 °C for 20 min. Ebselen was removed from the LDL using gel filtration as described above.

The oxidation process was performed in a thermostated waterbath at 37 °C in open vials with gentle shaking. To ensure sufficient oxygen availability for lipid hydroperoxide production at relatively high LDL concentrations (about 2 μM LDL), finely dispersed oxygen bubbles were carefully bubbled in so as to avoid sample denaturation at the air−liquid interface.

At certain stages throughout the oxidation process (observation points I−IV, as indicated in the inset to Figure 1), samples were withdrawn and 10 μL of 10 mM EDTA was added to inhibit copper-induced oxidation by chelation (*24*). AAPH-dependent oxidation was terminated by cooling to 4 °C and passage of the reaction mixture over a desalting column (Econo Pac 10DG, Bio-Rad); removal of water-soluble products by passage over a desalting column revealed that some 80% of the total TBARS, which is directly related to the MDA content of LDL particles, was released into the aqueous phase. Diene accumulation and TBARS formation explicitly verified the progression of lipid peroxidation at relatively high LDL concentrations.

Termination of the peroxidation process was proven by constant absorbance at 234 nm. The partially oxidized samples were stored in the dark at 4 °C until further analysis.

Differential Scanning Calorimetry. Calorimetric experiments were performed as described previously (*11*). In brief, a high-sensitivity adiabatic scanning microcalorimeter DASM-4 (Biobribor, Pushtchino, Russia) designed in 1978 by Privalov (*33*) was operated at a heating rate of 1 °C/min. The cells were maintained under about 250 kPa nitrogen pressure to avoid air bubble formation. The reference cell was filled with phosphate-buffered saline, since we have observed that the addition of copper or EDTA caused no alteration in the baseline profile. Heat capacity functions, $C_p(T)$, were obtained after subtraction of the buffer baseline and mass normalization of the experimental data. The thermotropic transition midpoint temperature, T_m, was taken as the temperature of the maximum of excess heat capacity. The corresponding calorimetric enthalpies (ΔH_{cal}) were calculated by integration of peak areas using spline-baseline extrapolation of the portions of the data below and above the peak transition. Some inaccuracy is involved in determination of the absolute values in oxidatively modified samples, since the transition peaks became rather broad as expressed in the transition half-width ($\Delta T_{1/2}$), thereby compromising precise estimation of the onset of melting relative to baseline. The cooperativity of the unfolding process was estimated from the ratio of the van't Hoff enthalpy (ΔH_{vH}) to the calorimetric enthalpy, according to the formula described by Sturtevant (*34*).

Oxidation Steps. Native LDL subspecies were taken as the reference for the baseline values and are referred to as point 0 (inset, Figure 1). Point I is situated at the end of the period corresponding to the lag phase, when antioxidants are consumed (*12*) but at which time only minor amounts of lipid peroxidation products can be detected. After depletion of all endogenous antioxidants, the radical chain reaction commences and the PUFAs (present in CE, phospholipids, and TG) are progressively oxidized to lipid hydroperoxides. During this propagation phase and when the production rate of dienes had attained its maximum, a second sample was withdrawn; this stage is referred to as point II. When the highest concentration of conjugated dienes was reached, point III was selected. Finally, point IV represents the phase of the decomposition period at which the concentration of aldehydes was maximal.

*Statistical Analysis.*The calorimetric values for native and oxidized LDL subspecies were compared by the Mann−Whitney test. Significance was taken at P values < 0.05.

RESULTS

For the calorimetric experiments, lipoprotein subspecies were isolated from the plasma of each of seven donors by density gradient centrifugation; our investigations were focused on LDL subspecies of intermediate density (d 1.030−1.040 g/mL). The use of LDL subspecies of intermediate density, where almost 50% of total plasma LDL mass was found in this density range (*23*, *35*), has the advantage of a markedly greater degree of homogeneity in physical and chemical properties, thus yielding representative, characteristic transition peaks by calorimetry.

LDL exhibits two endothermic transitions with transition temperatures centered at 20−35 °C and at about 80 °C, respectively. The first one arises from the reversible melting of the core-located lipids, while the second is associated with the irreversible unfolding and denaturation of apo-B100 (*16*, *36*). The thermotropic properties of apo-B100 unfolding appear different from that of typical globular proteins in that the enthalpic value calculated per gram of apo-B100 is only about 10% of that obtained for globular proteins. Representative calorimetric curves for native LDL and for the time course of copper-mediated oxidation are shown in Figure 1.

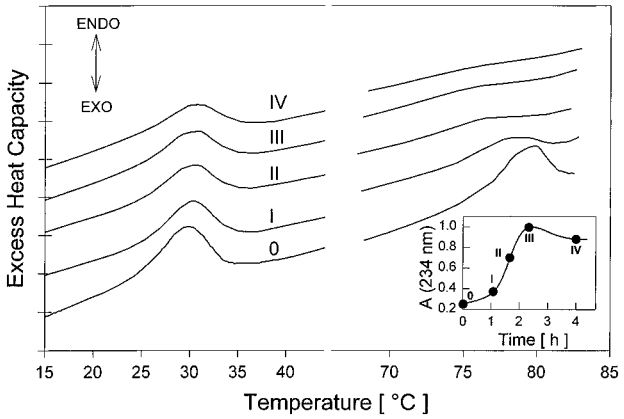

FIGURE 1: Representative DSC thermograms (baseline-subtracted but not normalized) for native LDL (curve 0) and the partially copper-oxidized preparations (curves I−IV). LDL concentration was about 5 mg/mL. Raw data were recorded from 1 to 95 °C at a heating rate of 1 °C/min. Reversibility of the core lipid transition was assessed upon heating to 45 °C, cooling to 0 °C, equilibration for 15 min, and reheating. Consecutive scans largely superimpose. The high-temperature peak, corresponding to thermal unfolding of apo-B100, resulted in irreversible protein precipitation. Prior to calorimetric experiments, progression of oxidation was stopped by adding 10 μL of 10 mM EDTA. The different time periods are referred to as points I−IV and are schematically depicted in the inset. (Inset) Typical time course of copper-mediated oxidation as obtained by continuously monitoring the changes in absorbance at 234 nm. Oxidation was performed in the presence of 0.1 μM LDL and 1.7 μM $CuCl_2$.

Table 1: Spectrophotometric Data on LDL Subspecies[a]

oxidation time course[b]	copper: diene (μmol/g of LDL)	copper: TBARS (μmol/g of apo-B)	AAPH[c] diene (μmol/g of LDL)
0	0	2.1 ± 0.1	0
I	14.2 ± 2.1	10.2 ± 2.0	10.1 ± 2.7
II	59.0 ± 12.5	13.5 ± 1.2	56.8 ± 2.7
III	104.4 ± 19.3	19.2 ± 3.8	97.1 ± 5.3
IV	89.5 ± 17.5	29.8 ± 4.5	ND[d]

[a] Density was 1.03−1.04 g/mL. The values are means ± SD of three subjects. [b] See inset to Figure 1 and Materials and Methods section. [c] TBARS are not detectable in AAPH-treated LDL as a result of dilution during desalting. [d] Not determined.

As a prelude to the calorimetric studies, we compared the effect of Cu- and AAPH-induced oxidation on the lipid moiety of LDL. Defined points on the diene production curve designated as I−IV were chosen according to criteria described in the Materials and Methods section and schematically depicted in the inset to Figure 1. A summary of the UV spectrophotometric results is given in Table 1. In addition, the time course of the diminution in the mass of the various lipid classes, expressed as a percentage of the initial mass, was followed during copper-induced oxidation (Table 2).

Influence of Copper- and AAPH-Induced Oxidation on the Core Lipid Transition in LDL. The midpoint temperatures

Table 2: Decrease of Lipids during Copper-Mediated Oxidation of LDL Subspecies[a]

	oxidation time course[b] (% of initial value)				
	0	I	II	III	IV
free cholesterol	100	96.9	99.1 ± 4.3	87.9 ± 5.6	76.2 ± 6.1
cholesteryl esters	100	92.8	90.9 ± 10.3	59.8 ± 24.8	46.0 ± 33.4
phospholipids	100	90.8	84.7 ± 12.6	68.6 ± 9.5	56.3 ± 8.5
triglycerides	100	89.4	82.7 ± 15.9	83.8 ± 28.6	84.0 ± 44.1

[a] Density was 1.03−1.04 g/mL. The values are mean ± SD of one determination for LDL preparations isolated from three subjects. Analysis was performed as described in Materials and Methods. [b] See inset to Figure 1 and Materials and Methods section.

of the order/disorder transition of the core lipids in native LDL varied between 28.4 and 31.5 °C. These values were based on a relatively high ratio of cholesteryl ester to triglyceride (9−15 mol of CE/mol of TG), a parameter that constitutes a major determinant of the actual melting temperature (*16*). Upon addition of copper ions, a slight but significant increase in T_m relative to that of native LDL (ΔT_m=0.5 ± 0.3 °C, $P < 0.02$) was observed in all preparations at the end of the lag period (point I) and remained almost constant during the propagation phase. As oxidation progressed, the peak gradually broadened; indeed, the transition half width, $\Delta T_{1/2}$, increased significantly from 6.2 ± 0.6 °C for the native sample to 8.5 ± 2.0 °C during the decomposition phase ($P < 0.05$). It is noteworthy that at advanced stages of oxidation (8 and 24 h), which involve extensive lipid depletion and decomposition, the core lipid transition peak was still detectable; however, as a consequence of the enhanced peak broadening, no quantitative evaluation was performed. Similar calorimetric transition characteristics were obtained for the AAPH-mediated oxidation system. After a short period of exposure, no significant effects on the melting behavior of the core lipids could be observed. At the end of the lag phase, T_m was decreased (ΔT_m = 1.8 ± 0.6 °C); simultaneously, the peak became broader.

Thermodynamic data representative for one donor and mean values for six different donors are presented in Table 3. The enthalpy values for the native LDL samples (ΔH_{cal} = 3.3 ± 1.0 J/g of CE) were within the range expected for LDL subspecies of intermediate density (*11*). Upon oxidation, CEs were progressively degraded and contributed to a lesser degree to the thermotropic transition. For a constant CE content, however, the calorimetric enthalpies remained constant during lag and propagation phase (ΔH_{cal} = 3.1 ± 0.4 J/g of CE, $P < 0.07$) and slightly, but not significantly increased during decomposition (ΔH_{cal} = 3.4 ± 0.5 J/g of CE, $P < 0.2$).

On reheating of LDL, no further alterations in the calorimetric parameters were detectable, thereby verifying the reversibility of the core lipid transition.

Influence of Oxidation on the Thermal Behavior of apo-B100. The precise midpoint temperatures for the irreversible protein transition varied between 78.1 and 79.9 °C (T_m = 79.3 ± 0.8 °C) for the individual native LDL samples; the associated calorimetric enthalpies were found to be ΔH_{cal} = 2.4 ± 0.2 J/g of apo-B100.

From initiation by incubation with copper ions to propagation, a significant decrease in T_m of 1.3 ± 0.6 °C ($P < 0.02$) was observed; simultaneously, the calorimetric enthalpy was reduced to about 55−60% of the initial value (ΔH_{cal} = 1.4 ± 0.5 J/g of apo-B100; $P < 0.003$) while the half-width of the transition, $\Delta T_{1/2}$, [$\Delta(\Delta T_{1/2})$ = 3.2 ± 1.5 °C] increased dramatically (Table 3). Even brief exposure (2−10 min) to copper ions resulted in a reduction in T_m of 1.5 ± 0.1 °C, in broadening of the peak and in marked lowering of the calorimetric enthalpy (approximately ≈25%). Quantitation of the calorimetric transition parameters at advanced stages of copper-induced oxidation (points III and IV, respectively) could not be performed due to extensive peak broadening. When AAPH was used as a prooxidant, then T_m decreased from 79.1 ± 0.75 °C for the native LDL preparations to 78.5 ± 0.7 °C after 10 min of AAPH exposure and finally, at the end of the lag time, to 77.0 ± 0.8 °C. Simultaneous with such changes, the transition peak broadened and the enthalpy diminished [i.e., ΔH_{cal} = 1.9 J/g of apo-B100 (for native LDL) to ΔH_{cal} = 0.4 J/g of apo-B100 (for samples at the end of the lag phase)]. For the early stages of copper- and free radical-driven oxidation, direct comparison of prooxidant effects on the heat capacity functions for protein unfolding are presented in Figure 2 and summarized in Table 4.

Table 3: Calorimetric Behavior of LDL Subspecies[a] during Copper-Mediated Oxidation

	oxidation time course[b]				
	0	I	II	III	IV
			Core Melting[c]		
T_m (°C)	28.6	29.2	29.2	29.1	29.5
$\Delta T_{1/2}$ (°C)	5.8	5.9	6.9	7.9	9.8
average[d]	6.2 ± 0.6	6.3 ± 1.0	6.7 ± 1.1	7.5 ± 1.4	8.5 ± 2.0
ΔH_{cal} (J/g of CE)	3.0	2.7	3.1	2.9	3.3
average	3.3 ± 0.8	2.9 ± 0.3	3.0 ±0.3	3.2 ± 0.4	3.4 ± 0.5
			Protein Denaturation[c]		
T_m (°C)	78.1	76.7	75.4		
average	79.3 ± 0.8	78.1 ± 1.2	77.8 ± 1.3		
$\Delta T_{1/2}$ (°C)	3.6	8.6	9.6		
ΔH_{cal} (J/g of apo-B100)	2.3	1.3	1.0		
average	2.4 ± 0.2	1.4 ± 0.5	1.0 ± 0.1		
ΔH_{cal} (%)	100	54.5	44.5		
ΔHvH/ΔH_{cal}[e]	0.8	1.4	1.5		
average	1.0 ± 0.1	1.7 ± 0.3	2.0 ± 0.3		

[a] Density was 1.03−1.04 g/mL. [b] See inset to Figure 1 and Materials and Methods section. [c] Calorimetric parameters are representative of data obtained for LDL from one donor. [d] Average values represent the means for analyses of LDL from six different donors. [e] Calculated according to the van't Hoff equation (*60*).

Due to the irreversibility of the apo-B100 unfolding process, thermodynamic equilibrium conditions are not provided. Hence, the excess heat capacity functions may not be strictly interpreted in terms of the van't Hoff equation. Nonetheless, the pronounced differences detected in the unfolding characteristics of apo-B100 in native and oxidized LDL justified the use of such an approach. For native LDL, the cooperativity of the unfolding process was close to unity ($\Delta H_{vH}/\Delta H_{cal}$ = 1.0 ± 0.1), resembling a two-state transition. By contrast, calorimetric data for modified LDL clearly reflect the status of an unfolded and partially denatured protein ($\Delta H_{vH}/\Delta H_{cal}$ = 1.7 ± 0.3 within the propagation phase).

DISCUSSION

We have demonstrated that oxidative modification of apo-B100 in native LDL particles of highly defined physico-

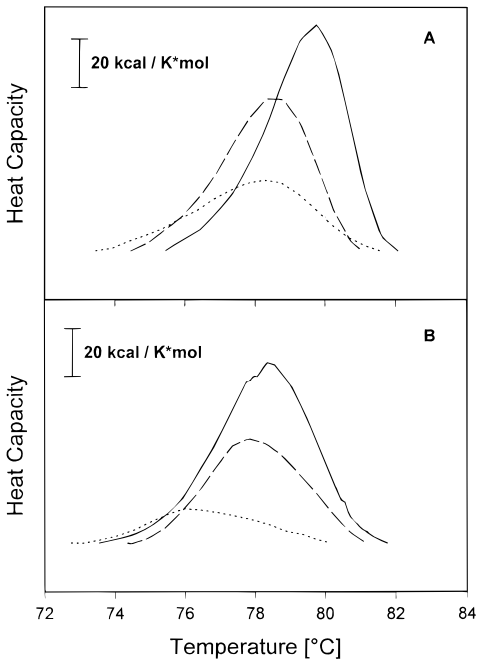

FIGURE 2: Heat capacity functions of thermal destabilization of apo-B100. Oxidation was initiated either by copper (A) or by AAPH (B). Buffer baselines were subtracted and subsequently the data were normalized to protein concentration, which was about 1 mg/mL. A slight variation in transition temperature for native LDL samples (solid lines) is typical for different donors. (A) The effect of copper-mediated oxidation was monitored after 2 min of exposure (dashed line) and at the end of the lag period (dotted line), oxidation was stopped by addition of EDTA. (B) AAPH-induced oxidation was terminated by cooling to 4 °C, followed by passage over a desalting column, after 10 min (dashed line) and at the end of the lag phase (dotted line).

Table 4: Calorimetric Data on Apo-B100 Denaturation at Early Stages of Copper- and AAPH-Induced Oxidation of LDL

	copper			AAPH		
oxidation time course[a]	0	0/I[b]	I	0	0/I	I
T_m (°C)	79.8	78.4	78.3	78.4	77.9	76.1
$\Delta T_{1/2}$ (°C)	2.6	3.0	3.8	3.3	3.3	3.7
ΔH_{cal} (J/g of apo-B100)	2.0	1.5	0.9	1.9	1.1	0.4
ΔH_{cal} (%)	100	75.0	44.4	100	57.9	21.1

[a] See inset to Figure 1 and Materials and Methods section. [b] Oxidation was terminated after 2 and 10 min of incubation with copper and AAPH, respectively, and corresponds to 2% and 14% of the respective lag periods.

chemical properties occurs independently of core lipid structure. Furthermore, protein damage was found to constitute an early event in oxidation, whereas the core lipid components preserve their structural integrity for a prolonged period. Protein destabilization was independent of the initiating agent (metal ions or a free radical generator). As metal ions are tightly bound to the LDL surface (*28*, *37*, *38*) presumably as a result of the formation of co-ordination complexes with amino acid residues at various sites along the protein chain (*39*), we interprete our results to indicate that the thermal protein destabilization is intimately linked to copper binding and reduction of Cu(II) to Cu(I) (*40*, *41*). A decrease in T_m and ΔH_{cal}, respectively, which indicates an unfolding in some regions of apo-B100 was observed even at the initial phase of copper oxidation. Further evidence that specific amino acid residues of apo-B100 are highly sensitive to copper ion attack derives from fluorescence studies, which reveal a significant decrease in the fluorescence intensity of tryptophan within a short period of exposure (*42*, *43*). However, when LDL was exposed to a steady flux of peroxyl radicals generated thermally by a water-soluble azo compound such as AAPH (*44*−*47*), then the initial loss in thermal stability of apo-B100 has to be explained either by direct attack at amino acid residues by free organic radicals or by reaction of such residues with decomposition products of preformed lipid hydroperoxides (*48*). We could show that elimination of lipid hydroperoxides by conversion to the corresponding hydroxides with ebselen (*32*) had no significant effect on the progression of protein damage (data not shown). Our results clearly indicate that specific changes in apo-B100 structure result in partial protein unfolding and enhanced protein aggregation at initial stages of oxidative stress. These findings lead us to the assumption that modifications in lipid−protein interaction occurred, involving exposure of previously buried hydrophobic regions of the polypeptide chain to the aqueous environment (*49*) and thus rendering them more accessible to oxidative attack. Indeed, it has been proposed that apo-B100 is wrapped around the outer surface of the LDL particle (*50*−*52*) with hydrophobic segments immersed in the hydrocarbon chain region of the phospholipid monolayer (*53*); and hydrophobic domains have been shown to be attacked preferentially upon oxidation (*54*).

The complete loss of the cooperatively folded domains of apo-B100 during the propagation phase of the radical chain reaction is probably caused by reactive lipid breakdown products, such as peroxyl and alkoxyl radicals, which can induce continuous modification of its primary structure. Thus, His and Pro residues are converted to Asp and Glu (*55*), and derivatization of accessible ϵ amino acid groups leads to a progressive decrease in trinitrobenzenesulfonic acid (TNBS) reactivity (*56*). Accordingly, cross-linking reactions involving secondary oxidation products, such as reactive aldehydes, in addition to protein cleavage or aggregation (*37*, *57*) must be taken into account. The equilibrium between fragmentation on the one hand and cross-linking of polypeptide chains on the other depends on the arrangement of the lipid chains within the particle (*58*) but may also reflect a close association of the hydrophobic domains of the protein with the lipid environment, thus facilitating the interaction of apo-B100 with secondary lipid peroxidation products.

During the early phase of oxidation, we observed that phospholipids and cholesteryl esters are degraded approximately in proportion to their content of polyunsaturated fatty acids. As LDL particles contain about 3 times more bisallylic hydrogen groups within the neutral core than in the polar phospholipid shell (*12*, *37*), the involvement of rapid radical transfer mechanisms must be considered. Thus, differences between the mobilities of radicals in the outer layer as compared to the core of LDL favour transfer from the surface to the core, and in turn hydrophilic peroxidation products are released from the inner core to the surface. Lipid peroxidation progressively reduces the content of polyunsaturated cholesteryl arachidonate and linoleate and results in a decrease in lipoprotein fluidity and an increase in membrane rigidity (*59*). Under these conditions, an enhancement of core stability may be predicted and is entirely consistent with the slight increase in melting temperature that we observed at the onset of oxidation. Furthermore, if

water-soluble oxidation products of the core PUFAs are released to the aqueous medium, the peak of the thermal transition became even sharper as compared to the native sample, implying an enhanced cooperativity within the core environment. Equally, our results reveal that some features of the organized lipid arrangement are preserved even after extensive oxidation. Indeed, the order/disorder transition of the core lipids, which is assumed to be a determinant parameter for antioxidant efficiency and susceptibility of lipids to oxidation (*11*), was maintained during the time course of oxidation.

In conclusion, the present calorimetric studies reveal that the initial oxidative changes in LDL particles are focused on the structure and organization of the protein moiety, i.e., apo-B100. Moreover, such effects are independent of the nature of the prooxidant agent, i.e., Cu^{2+} or AAPH, and precede oxidative modification of lipid components. Clearly, then, the loss in protein stability constitutes a key step in the sequence of structural modification, which leads to the deviation of LDL uptake by the nonatherogenic LDL receptor pathway to that by the scavenger receptors in monocyte-derived macrophages; this latter step represents an essential stage in the formation of macrophage foam cells, a principal characteristic of human atherosclerotic plaques. Such studies should identify new therapeutic mechanisms for the prevention of LDL−apo-B100 oxidation during the atherogenic process.

ACKNOWLEDGMENT

We are indebted to M. Zechner for expert technical assistance.

REFERENCES

1. Haberland, M. E., Fong, D., and Cheng, L. (1988) *Science 241*, 215−218.
2. Steinberg, D., Parthasarathy, S., Carew, S., Khoo, J. C., and Witztum, J. L. (1989) *New Engl. J. Med. 320*, 915−924.
3. Steinbrecher, U. P., and Zhang, H. (1990) *Free Rad. Biol. Med. 9*, 155−168.
4. Witztum, J. L., and Steinberg, D. (1991) *J. Clin. Invest. 88*, 1785−1792.
5. Ylä-Herttuala, S. (1991) *Ann. Med. 23*, 561−567.
6. Dejager, S., Bruckert, E., and Chapman, M. J. (1993) *J. Lipid Res. 34*, 295−308.
7. Tribble, D. L., Holl, L. G., Wood, P. D., and Krauss, R. M. (1992) *Atherosclerosis 93*, 189−199.
8. De Graaf, J., Hak-Lemmers, H. L. M., Hectors, M. P. C., Demacker, P. N. M., Hendriks, J. C. M., and Stalenhoef, A. F. H. (1991) *Arterioscler. Thromb. 11*, 298−306.
9. Lund-Katz, S., Ibdah, J. A., Letizia, J. Y., Thomas, M. T., and Phillips, M. C. (1988) *J. Biol. Chem. 263*, 13831−13838.
10. Esterbauer, H., Dieber-Rotheneder, M., Waeg, G., Striegl, G., and Jürgens, G. (1990) *Chem. Res. Toxicol. 3*, 77−92.
11. Schuster, B., Prassl, R., Nigon, F., Chapman, M. J., and Laggner, P. (1995) *Proc. Natl. Acad. Sci. U.S.A. 92*, 2509−2513.
12. Esterbauer, H., Gebicki, J., Puhl, H., and Jürgens, G. (1992) *Free Rad. Biol. Med. 13*, 341−390.
13. Deckelbaum, R. J., Shipley, G. G., Small, D. M., Lees, R. S., and George, P. K. (1975) *Science 190*, 392−394.
14. Atkinson, D., Deckelbaum, R. J., Small, D. M., and Shipley, G. G. (1977) *Proc. Natl. Acad. Sci. U.S.A. 74*, 1042−1046.
15. Laggner, P., and Müller, K. (1978) *Q. Rev. Biophys. 11*, 371−425.
16. Deckelbaum, R. J., Shipley, G. G., and Small, D. M. (1977) *J. Biol. Chem. 252*, 744−754.
17. Laggner, P., Kostner, G. M., Rakusch, U., and Worcester, D. L. (1981) *J. Biol. Chem. 256*, 11832−11839.
18. Laggner, P., Kostner, G. M., Degovics, G., and Worcester, D. L. (1984) *Proc. Natl. Acad. Sci. U.S.A. 81*, 4389−4393.
19. Jürgens, G., Lang, G., and Esterbauer, H. (1986) *Biochim. Biophys. Acta 875*, 103−114.
20. Palinski, W., Rosenfeld, M. E., Ylä-Herttuala, S., Gurtner, G. C., Socher, S. S., Butler, S. W., Parthasarathy, S., Carew, T. E., Steinberg, D., and Witztum, J. L. (1989) *Proc. Natl. Acad. Sci. U.S.A. 86*, 1372−1376.
21. Steinbrecher, U. P. (1987) *J. Biol. Chem. 262*, 3603−3608.
22. Chapman, M. J., Goldstein, S., Lagrange, D., and Laplaud, P. M. (1981) *J. Lipid Res. 22*, 339−358.
23. Chapman, M. J., Laplaud, P. M., Luc, G., Forgez, P., Bruckert, E., Goulinet, S., and Lagrange, D. (1988) *J. Lipid Res. 29*, 442−458.
24. Esterbauer, H., Striegl, G., Puhl, H., and Rotheneder, M. (1989) *Free Rad. Res. Commun. 6*, 67−75.
25. Kleinveld, H. A., Hak-Lemmers, H. L. M., Stalenhoef, A. F. H., and Demacker, P. N. M. (1992) *Clin. Chem.* 38, 2066−2072.
26. Puhl, H., Waeg, G., Tatzber, F., and Esterbauer, H. (1993) in *Free Radicals: From Basic Science to Medicine* (Poli, G., Albano, E., and Dianzani, M. U., Eds.) pp 479−489, Birkhäuser Verlag, Basel, Switzerland.
27. Kritharides, L., Jessup, W., Gifford, J., and Dean, R. T. (1993) *Anal. Biochem. 213*, 79−89.
28. Gieseg, S. P., and Esterbauer, H. (1994) *FEBS Lett. 343*, 188−194.
29. Gutteridge, J. M. C., and Halliwell, B. (1990) *Trends Biochem. Sci. 15*, 129−135.
30. Halliwell, B. (1990) *Free Rad. Res. Commun. 9*, 1−32.
31. Kuksis, A., Myher, J. J., Maral, L., and Geher, K. (1975) *J. Chromatogr. Sci 13*, 423−430.
32. Sattler, W., Maiorino, M., and Stocker, R. (1994) *Arch. Biochem. Biophys. 309*, 214−221.
33. Privalov, P. L. (1980) *Pure Appl. Chem. 52*, 479−497.
34. Sturtevant, J. M. (1974) *Annu. Rev. Biophys. Bioeng. 3*, 35−51.
35. Nigon, F., Lesnik, P., Rouis, M., and Chapman, M. J. (1991) *J. Lipid Res.* 32, 1741−1753.
36. Walsh, M. T., and Atkinson, D. (1990) *J. Lipid Res. 31*, 1051−1062.
37. Sattler, W., Kostner, G. M., Waeg, G., and Esterbauer, H. (1991) *Biochim. Biophys. Acta 1081*, 65−74.
38. Kuzuya, M., Yamada, K., Hayashi, T., Funaki, C., Naito, M., Asai, K., and Kuzuya, F. (1992) *Biochim. Biophys. Acta 1123*, 334−341.
39. Simpson, J. A., and Dean, R. T. (1990) *Free Rad. Res. Commun. 10*, 303−312.
40. Lynch, S. M., and Frei, B. (1995) *J. Biol. Chem. 270*, 5158−5163.
41. Kontush, A., Meyer, S., Finckh, B., Kohlschutter, A., and Beisiegel, U. (1996) *J. Biol. Chem. 271*, 11106−11112.
42. Vanderyse, L., Devreese, A. M., Baert, J., Vanloo, B., Lins, L., Ruysschaert, J. M., and Rosseneu, M. (1992) *Atherosclerosis 97*, 187−199.
43. Giessauf, A., Steiner, E., and Esterbauer, H. (1995) *Biochim. Biophys. Acta 1256*, 221−232.
44. Yamamoto, Y., Haga, S., Niki, E., and Kamiya, Y. (1984) *Bull. Chem. Soc. Jpn. 57*, 1260−1264.
45. Noguchi, N., Gotoh, N., and Niki, E. (1993) *Biochim. Biophys. Acta 1168*, 348−357.
46. Thomas, M. J., Thornburg, T., Manning, J., Hooper, K., and Rudel, L. L. (1994) *Biochemistry 33*, 1828−1834.
47. Gaziano, J. M., Hatta, A., Flynn, M., Johnson, E. J., Krinsky, N. I., Ridker, P. M., Hennekens, C. H., and Frei, B. (1995) *Atherosclerosis 112*, 187−195.
48. Maiorino, M., Zamburlini, A., Roveri, A., and Ursini, F. (1995) *Free Rad. Biol. Med. 18*, 67−74.
49. Haberland, M. E., Olch, C. L., and Folgelman, A. M. (1984) *J. Biol. Chem. 259*, 11305−11311.

50. Chatterton, J. E., Schlapfer, P., Bütler, E., Gutierrez, M. M., Puppione, D. L., Pullinger, C. R., Kane, J. P., Curtiss, L. K., and Schumaker, V. N. (1995) *Biochemistry 34*, 9571−9580.
51. Chatterton, J. E., Phillips, M. L., Curtiss, L. K., Milne, R. W., Marcel, Y. L., and Schumaker, V. N. (1991) *J. Biol. Chem.* 266, 5955−5962.
52. Schumaker, V. N., Phillips, M. L., and Chatterton, J. E. (1994) *Adv. Protein Chem. 45*, 205−248.
53. Yang, C.-Y., Kim, T. W., Pao, Q., Chan, L., Knapp, R. D., Gotto, A. M., Jr., and Pownall, H. J. (1989) *J. Prot. Chem. 8*, 689
54. Singh, S., Suri, R., and Agrawal, C. G. (1995) *Biochim. Biophys. Acta 1254*, 135−139.
55. Stadtman, E. R. (1992) *Science 257*, 1220−1224.
56. Lesnik, P., Dentan, C., Vonica, A., Moreau, M., and Chapman, M. J. (1995) *Arterioscler., Thromb., Vasc. Biol. 15*, 1−10.
57. Schuh, J., Fairclough, G. F., and Haschemayer, R. H. (1978) *Proc. Natl. Acad. Sci. U.S.A. 75*, 3173−3177.
58. Dean, R. T., Gieseg, S., and Davies, M. J. (1993) *Trends Biochem. Sci. 18*, 437−441.
59. Berlin, E., and Young, C. J. (1983) *Atherosclerosis 48*, 15−27.
60. Mabrey, S., and Sturtevant, J. M. (1978) in *Methods in Membrane Biology* (Kern, E. D., Ed) pp 237−244, Plenum Press, New York.

BI971853F